Int J Fract (2008) 154:131–145
DOI 10.1007/s10704-009-9317-8

ORIGINAL PAPER

Statistics of strength of ceramics: finite weakest-link model and necessity of zero threshold

Sze-Dai Pang · Zdeněk P. Bažant · Jia-Liang Le

Received: 21 July 2008 / Accepted: 15 January 2009

Abstract It is argued that, in probabilistic estimates of quasibrittle structure strength, the strength threshold should be considered to be zero and the distribution to be transitional between Gaussian and Weibullian. The strength histograms recently measured on tough ceramics and other quasibrittle materials, which have been thought to imply a Weibull distribution with nonzero threshold, are shown to be fitted equally well or better by a new weakest-link model with a zero strength threshold and with a finite, rather than infinite, number of links in the chain, each link corresponding to one representative volume element (RVE) of a non-negligible size. The new model agrees with the measured mean size effect curves. It is justified by energy release rate dependence of the activation energy barriers for random crack length jumps through the atomic lattice, which shows that the tail of the failure probability distribution should be a power law with zero threshold. The scales from nano to macro are bridged by a hierarchical model with parallel and series couplings. This scale bridging indicates that the power-law tail with zero threshold is indestructible while its exponent gets increased on each passage to a higher scales. On the structural scale, the strength distribution except for its far left power-law tail, varies from Gaussian to Weibullian as the structure size increases. For the mean structural strength, the theory predicts a size effect which approaches the Weibull power law asymptotically for large sizes but deviates from it at small sizes. This deviation is the easiest way to calibrate the theory experimentally. The structure size is measured in terms of the number of RVEs. This number must be convoluted by an integral over the dimensionless stress field, which depends on structure geometry. The theory applies to the broad class of structure geometries for which failure occurs at macro-crack initiation from one RVE, but not to structure geometries for which stability is lost only after large macro-crack growth. Based on tolerable structural failure probability of $<10^{-6}$, the change from nonzero to zero threshold may often require a major correction in safety factors.

Keywords Size effect · Fracture mechanics · Statistical strength · Activation energy · Atomic lattice · Quasibrittle materials

S.-D. Pang
Department of Civil Engineering, National University of Singapore, Kent Ridge, Singapore

Z. P. Bažant (✉)
Northwestern University, Evanston, USA
e-mail: z-bazant@northwestern.edu

J.-L. Le
Department of Civil and Environmental Engineering, Northwestern University, Evanston, USA

1 Introduction

As generally agreed (Duckett 2005; Melchers 1987; NKB 1978), engineering structures must be designed

for failure probability $P_f \leq 10^{-6}$ per lifetime. For such a probability limit, structural failures are so rare that they do not appreciably contribute to other risks that people willingly or inevitably face.

In the limiting special cases of plastic or brittle failure, it is not difficult to ensure this probability limit because the type of probability distribution of structural strength is known and calculation of the mean and variance suffices to calibrate the entire distribution, including the tail. For plastic (or ductile) failures, the strength of all the representative material volumes (RVEs) along the failure surface is mobilized simultaneously, and so the failure load P must be a weighted sum of the strength contributions from all the RVEs, which are random. According to the central limit theorem (Bouchaud and Potters 2000; Bulmer 1979; Ang and Tang 1984), a sum of independent random variables of arbitrary distributions rapidly converges to the Gaussian (or normal) distribution, and so the plastic failure load must inevitably follow the Gaussian distribution. Brittle failures are those in which the failure of one RVE causes the whole structure to fail. Hence, the weakest-link model applies, and if the number of RVEs that could trigger the failure is very large, the Weibull distribution must apply (as a consequence of the stability postulate of extreme value statistics (Ang and Tang 1984; Gumbel 1958)).

Figure 1 compares the Gaussian and Weibull cumulative distribution functions (cdf) for the same mean and the same typical coefficient of variation. Note that, within the probability range of about 3–97%, these cdf's differ very little (and thus are barely distinguishable in strength histograms with less than about 500 tests). However, the situation is completely different in the far-left tail. The point of failure probability 10^{-6} is seen to lie, for the Weibull distribution, almost twice as far from the mean than it does for the Gaussian distribution. This means that, relative to the standard deviation, the safety factor for brittle failures must be about twice as large as that for ductile failures.

Quasibrittle materials, such as tough ceramics, are brittle heterogeneous materials in which the fracture process zone (FPZ) (whose width is approximately equal to the RVE size) is not negligible compared to the structure size D. Aside from coarse-grained or toughened ceramics, these materials include concrete as the archetypical case, rocks, stiff soils, sea ice, snow slabs, fiber-polymer composites, rigid foams, wood, paper, many bio-materials (bone) and other materials on the micrometer scale (Bažant 2005; Bažant and Chen 1997). As the structure size D is increased, the behavior of these materials transits from quasi-plastic to brittle. This transition has been well justified theoretically (Bažant 1984, 2005; Bažant and Kazemi 1990) and is evidenced by the type 2 size effect law (Bažant 1984, 2004b, 2001; RILEM 2004). This law, amply verified experimentally, describes the curves of mean nominal structure strength σ_N versus structure size D for geometrically similar specimens with notches or large cracks; (see Fig. 1e and j-p in Bažant 2004b).

Consequently, the distribution of strength of quasibrittle structures must be expected to change from predominantly Gaussian to Weibullian as the structure size increases. Hence, the ratio of the safety factor to the standard deviation of σ_N is expected to nearly double when passing from small laboratory specimens to quasibrittle structures much larger than the RVE. Indirect experimental verification of such behavior has been provided for concrete and fiber composites (Bažant and Planas 1998), and the purpose of this study is to provide it for quasibrittle ceramics. Direct experimental verification of failure probability $\leq 10^{-6}$ by strength histograms is impossible (since $>10^8$ test repeats would be needed).

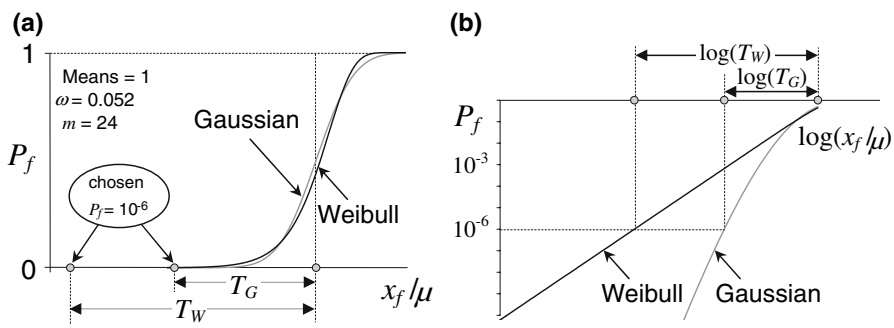

Fig. 1 Difference between points of $P_f = 10^{-6}$ for Gaussian and Weibull distributions

Formulation of the theory is facilitated by one remarkable feature that came to light recently (Bažant and Pang 2005, 2006, 2007): The rate processes such as the effects of temperature and activation energy on chemical reaction rates, phase changes, creep rates, dislocation mobility, etc., are not the only phenomena that translate simply and directly from the nano-scale to the continuum macro-scale of material. The tail of the cumulative distribution function (cdf) of failure probability versus strength is another such phenomenon, because two simple properties appear to be valid: (1) The left tail of cdf of strength on the atomic scale appears to be a power-law with a zero threshold; and (2) the power-law tail with zero threshold is indestructible and its exponent gets raised at when passing to higher scales. The present paper will explore the consequences of these two properties for the cdf of strength of structures consisting of tough ceramics.

Considered here will be only structures of positive geometry (Bažant 2005; Bažant and Planas 1998). This is the usual situation for ceramics, in which the derivative of stress intensity factor with respect to crack length at constant load is positive, causing failure under load control to occur as soon as the FPZ fully develops and the macro-crack initiates from one RVE. The statistics of strength of such structures follows the weakest-link chain model. If the number of links tends to infinity, this model leads, according to the stability postulate of extreme value statistics (Gumbel 1958; Ang and Tang 1984), to the Weibull distribution (which was actually first derived by Fisher and Tippett 1928).

Freudenthal (1968) proposed to justify the Weibull distribution of strength by statistics of microscopic material flaws. Implicit to his justification were three simplifying hypotheses: (1) If the structure is subdivided into many volume elements corresponding to the links of the weakest-link model, the largest flaw in each element obeys Cauchy-type distribution; (2) the flaws are non-interacting, i.e., the stress field of the flaw in one element does not affect the flaw in an adjacent element; and (3) the Griffith theory can be applied to the flaws to calculate the strength of each volume element. However, the stress fields around adjacent flaws do interact, and for very small flaws the cohesive crack model would be more realistic. Besides, there is no compelling physical reason for a Cauchy-type distribution (except that otherwise the hypothesis of flaws would not lead to the Weibull distribution). Furthermore, for materials such as concrete, which is totally disordered from the nanoscale up, there is an additional problem—the definition of flaws is ambiguous and subjective. So Freudenthal's theory is merely a macro-micro relationship useful for some brittle materials, but not a proof.

The two-parameter Weibull distribution, which has a zero strength threshold, was shown to fit the histograms of strength data for many fine-grained engineering ceramics (Gross 1996; Lohbauer et al. 2002; Santos et al. 2003; Salem et al. 1996; Okabe and Hirata 1995). However, for ceramic specimens not large enough compared to the grain size or the toughening zone, it was found that the Weibull distribution with a zero threshold cannot give a good fit of test data (Salem et al. 1996; Okabe and Hirata 1995). When the three-parameter Weibull distribution, having a finite threshold, was adopted, the histogram fits were found to improve. However, this was shown for only relatively small data sets (Gross 1996; Stanley and Inanc 1985; Duffy et al. 1993), and the corresponding size effect has not been checked.

For broad-range strength histograms with many thousands of data, the three-parameter Weibull distribution still shows a systematic deviation from the experimental histograms of cement mortar (see the refitting of Weibull's (Weibull 1939) data in Fig. 10 of Bažant and Pang 2007). This deviation is not surprising since the aforementioned new theory (Bažant and Pang 2007), based on the energy release effect on the activation energy barriers of the free energy potential of a fracturing atomic lattice block, indicates that the strength threshold ought to be zero.

According to that theory, the problem lies elsewhere —in the fact that the Weibull distribution corresponds to the weakest-link chain model in which the number of links tends to infinity. When the specimen is not large enough compared to the grain size, a chain with a finite number of links must be used. This appears to be a crucial point, which leads to a distribution that differs from Weibull's and has already been shown to yield excellent agreement with broad strength histograms for cement mortar (Bažant and Pang 2007). We will explore whether the same holds for ceramics.

The finite weakest-link model also yields good agreement with the experimental mean size effect curves (Bažant and Pang 2007). The size effect is defined as the dependence of nominal strength $\sigma_N = P/bD$ on structure size D when geometrically similar structures are compared; here b = structure width and P = maximum load (representing the failure load if

the load is controlled). If a deterministic failure criterion is specified in terms of stresses and strains, as in elasticity or plasticity, there is no size effect (Bažant 1984, 2004b; RILEM 2004). But if the failure criterion also involves fracture energy or a material characteristic length, e.g. (Bažant 2005; RILEM 2004), there is a size effect that can be explained energetically and represents a transition between small-size and large-size asymptotic power laws. If, in addition, the randomness of material strength is considered and if the failure can begin at various locations, the large-size asymptotic size effect becomes stronger (RILEM 2004; Bažant 2004b).

2 Conspectus of the theory

2.1 Failure probability tail on the atomic lattice scale

A theory justifying and quantifying the transition between Gaussian and Weibull cdf in terms of the statistics of failure on the atomic lattice level has recently been developed at Northwestern University. Initially a rather simplified argument was proposed on the basis of Maxwell–Boltzmann type statistics of the severance of bonds of atomic pairs due to stress dependence of the activation energy barriers (Bažant and Pang 2005, 2006, 2007). More recently, the distribution of strength of one RVE has been derived from fracture mechanics of propagation of a crack in an atomic lattice block (Bažant et al. 2008). In contrast to fracture mechanics of continuous bodies, the curve of the free energy potential Π of the block, versus displacement u due to fracture and elasticity of the lattice, does not decrease monotonically but consists of a series of metastable states which correspond to lengths jumps of the atomic lattice crack and are separated by activation energy barriers Q (Bažant et al. 2008). Because of thermal vibrations, the state of the lattice block, characterized by potential Π, can jump over these barriers, with a certain frequency. Since a change of crack length a by one atomic spacing h must cause only a small change in Π, the barrier of $Q_0 - \Delta Q/2$ of the atomic lattice block for the forward jumps (crack length increase) must be only slightly lower than the barrier $Q_0 + \Delta Q/2$ for the backward jumps (crack length shortening). So the jumps can occur both forward and backward, though not with the same frequencies. From fracture mechanics, it follows that (Bažant et al. 2008):

$$\Delta Q = h\left[\frac{\partial \Pi}{\partial a}\right]_P = hb\mathcal{G} = \sigma^2 V_a/E \tag{1}$$

$$V_a = hbD_a g(\alpha) \tag{2}$$

where $\mathcal{G}$ = energy release rate, σ = applied remote stress, P = load on the atomic lattice block; D_a, b = its cross section length and its width in the third dimension; E = Young's modulus of continuous approximation of the lattice, V_a = activation volume of lattice crack, $g(\alpha) = k^2(\alpha)$ = dimensionless energy release rate of the atomic lattice block as a function of relative crack length $\alpha = a/D_a$, and $k(\alpha)$ = dimensionless stress intensity factor. According to the transition-rate theory (Kaxiras 2003; Philips 2001), the frequencies of the forward and backward jumps are obtained from Kramer's formula as $v_a e^{-(Q_0 \pm \Delta Q)}/kT$ where v_a = constant, T = absolute temperature and k = Boltzmann constant (Risken 1989). Because $\Delta Q \ll Q_0$, the jumps must be happening in both the forward and backward directions, and what matters is the net frequency of jumps, which approximately is (Bažant et al. 2008):

$$f_b = C_f \sigma^2, \quad C_f = e^{-Q_0/kT} v_a V_a / EkT \tag{3}$$

which is justified by the fact that $V_a\sigma^2 \ll 2EkT$. For the foregoing derivation, it is also required that $\Delta Q \ll kT \ll Q_0$ or $\sigma \ll \sqrt{EkT/V_a}$. Furthermore, the crack front diffusion may be neglected due to large Péclet number.

The break frequency f_b, which is proportional to failure probability, was in previous simplified analysis (Bažant and Pang 2006, 2007) shown to depend linearly on stress at the scale of interatomic bonds. Is that a conflict with Eq. 3? No, since it was also shown that the passage to a higher scale, which involves strain compatibility conditions equivalent to parallel coupling, raises the exponent of the power-law tail of the cdf of strength. Thus, the rasing of the stress exponent from 1 to 2, in passing from atomic bond scale to lattice block scale, as seen in Eq. 3, is not inexplicable. The foregoing analysis implies that the left tail of strength cdf at nanoscale must be a power law.

2.2 Hierarchical Series-Parallel coupling model bridging nano to macro

It is generally accepted that, for the purpose of statistics, the transition from the nano-scale to the representative volume of material (RVE) on the macro-scale can be mechanically represented by series couplings (i.e. the

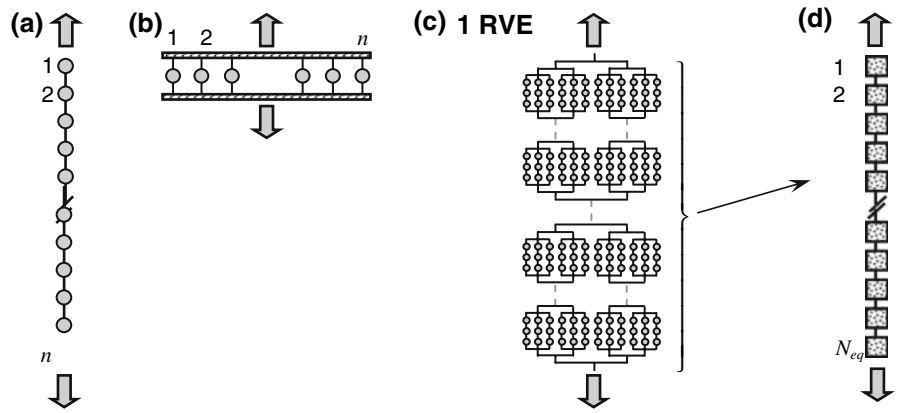

Fig. 2 Models of series and parallel couplings: **a** chain; **b** fiber bundle; **c** hierarchy of sub-chains and sub-bundles; **d** a weakest link model made up of elements, each representing a RVE

chain model) and parallel couplings (i.e. the fiber bundle model); Fig. 2. In passing to higher scales by means of parallel and series couplings, the power law tail with a zero threshold is indestructible, although its exponent increases (Bažant and Pang 2007).

For a chain of n elements (links) of random strength, all of which have a cdf with a power-law tail of exponent p, the cdf of the entire chain has also a power-law tail and its exponent is again p. If the tail exponents for different elements in the chain are different, it is the smallest one which is the exponent of the cdf tail of the entire chain.

For parallel coupling of elements of random strength (fiber bundle), one must first specify the load-sharing rule according to which the stresses are redistributed after one element attains its strength limit. Various empirical load-sharing rules have been considered in the literature, but it is more realistic to base load sharing on a mechanical model. Because generalization is obvious, it suffices to base load sharing on the hypothesis that all the fibers in the bundle to have equal elastic stiffness and are subjected to the same displacement. After reaching the strength limit, a fiber is considered to respond either in a brittle manner, in which case its stress drops suddenly to zero, or in a ductile (or plastic) manner, in which case the stress remains constant as the displacement increases.

If the fibers (or elements) have a cdf with a power-law tail of exponent p, then the cdf of strength of a bundle of n fibers is also a power law and has the exponent of np. More generally, unequal exponents of power-law cdf tails of elements coupled in parallel are additive. For plastic bundles, this remarkably simple property can be proven by asymptotic expansions of cdf (Bažant and Pang 2007) or through Laplace transform of cdf. For brittle bundles, this property was proven in (Phoenix et al. 1997; Harlow et al. 1983). A simpler proof (Bažant and Pang 2007) can be based on asymptotic expansion of the exact recursive equation for cdf derived by Daniel (Daniel 1945), who also showed that the cdf of a brittle bundle converges to the Gaussian distribution as $n \to \infty$. For a plastic bundle, such convergence is an obvious consequence of the central limit theorem of the theory of probability. The additivity of tail exponents appears to be also true for the intermediate case of fibers that exhibit gradual post-peak softening, although an analytical proof is lacking.

Regardless of the cdf of individual elements in a bundle, a parallel coupling of n elements produces for the bundle strength a cdf that converges to the Gaussian (or normal) distribution as $n \to \infty$. The power-law tail of the individual elements is always retained by a finite bundle but is rapidly pushed farther and farther out as n grows, and disappears only for $n \to \infty$. On the other hand, a series coupling of n elements having an arbitrary cdf with a power-law left tail produces for the chain a cdf in which a Weibull portion is spreading from left to right as $n \to \infty$, no matter how remote the power-law tail of the individual elements is. However, these observations need to be quantified.

The Weibull probability distribution with modulus m has a power-law tail of exponent m. According to laboratory tests on the RVE scale (macro-scale), the $m-$values typically range from 10 to 50. If the macro-scale exponent is, for instance, $m = 24$, one way to explain its value would, for instance, be a parallel coupling of 12 elements each of which has a cdf with the nano-scale tail exponent of 2. However, a serious problem with this explanation has been identified in (Bažant and Pang 2007)—the power-law tail of exponent 24

would extend only up the failure probability of $P_f = 10^{-22}$. For such a remote power-law tail, a completely Weibullian cdf would occur only if the structure contained about 10^{24} equivalent RVEs, each represented by one bundle. This would be an absurd idea. It means that no structure made of such material could ever exhibit Weibull strength statistics if the transition from the nano-scale to the RVE scale involved only parallel couplings. The fact that structures with more than 10^4 RVEs do exhibit Weibull distribution of strength implies that the power-law tail for one RVE must extend at least to $P_f \approx 10^{-4}$.

The reach of the power-law tail of the cdf of bundle strength diminishes rapidly with the increasing number of parallel fibers. It was shown that the length of power-law tail in terms of failure probability P_f decreases as $P_{t_n} \sim (P_{t_1}/n)^n - (P_{t_1}/3n)^n$ for brittle fibers, or as $(P_{t_1}/n)^n$ for plastic fibers (Bažant and Pang 2006, 2007), which is roughly by an order of magnitude for each additional fiber in the bundle. Hence, it may be concluded that, if one RVE were modeled by a bundle with more than 2 fibers of tail exponent >5, or with more than 3 fibers of tail exponent >2, the power-law tail would be so remote from the mean that the tail of cdf for a chain of RVEs would never exhibit the Weibull distribution, and thus would never apply to brittle or quasibrittle materials. On the other hand, modeling of an RVE by a bundle with only two fibers of tail exponent 2 is not possible since the resulting Weibull modulus m would be 4, which is unrealistic. For brittle materials, the Weibull modulus $m \approx 10$ to 50.

The series coupling has the opposite effect. In a chain of N elements, each of which has an arbitrary cdf onto which a power-law tail reaching up to $P_f = 0.001$ is grafted, the Weibull portion of the cdf of the chain reaches up to $P_f = 40\%$ when $N = 500$, and up to 99.99% when $N = 10^4$ (the tail is here considered Weibullian as long as the cdf of the chain does not deviate by more than 1%). Noting these features is crucial for realistic modeling of ceramics on the scale of normal application. When $N > 10^4$, the material behaves as perfectly brittle. Otherwise the chain is quasibrittle, since the fracture process zone is not negligibly small compared to the cross section size (Bažant and Planas 1998; Bažant and Chen 1997).

So it is inevitable to conclude that, if the power-law tail of one quasibrittle RVE should have an exponent between 10 and 50 and should extend up to failure probability between 0.0001 and 0.01, the transition from atomistic to macro-continuum scale must consist of parallel couplings of no more than two chains near the macro-scale, and not more than three near the atomistic scale. The chains must be long enough, or else the observations of Weibull distribution of strength on fine-grained ceramics, e.g. (Weibull 1939) could not be explained. Therefore, the nano-macro transition needs to be statistically represented by a hierarchical model of series and parallel couplings (Bažant and Pang 2005, 2006, 2007), as idealized in Fig. 2. Such a model may consist of bundles of 2 long chains, each consisting of sub-bundles of 2 or 3 long sub-chains, each consisting of sub-sub-bundles of sub-sub-chains, etc., until the scale of atomic lattice is reached. The bundles of chains (parallel couplings) serve to raise the exponent of the cdf tail, and long chains of bundles (series couplings) serve to lengthen the extent of the reach of power-law tail into higher P_f.

2.3 Grafted probability distribution for one RVE

At the level of one RVE, numerical simulations reveal that a transition from Weibull cdf to Gaussian cdf occurs smoothly but over a relatively short segment of cdf. In consequence, and for the sake of simplicity, we may consider a Weibull cdf to be grafted from the left onto a Gaussian cdf, with only the cdf value and slope being continuous through the grafting point (Bažant and Pang 2006, 2007). In terms of pdf (probability density function) $p_1(\sigma_N)$, which is the derivative of cdf,

$$\text{for } \sigma_N < \sigma_{N,gr}: \tag{4}$$
$$p_1(\sigma_N) = r_f \phi_W(\sigma_N) = r_f (m/s_1)(\sigma_N/s_1)^{m-1} \mathrm{e}^{-(\sigma_N/s_1)^m}$$

$$\text{for } \sigma_N \geq \sigma_{N,gr}: \tag{5}$$
$$p_1(\sigma_N) = r_f \phi_G(\sigma_N) = r_f \mathrm{e}^{-(\sigma_N-\mu_G)^2/2\delta_G^2}/(\delta_G\sqrt{2\pi})$$

Here m (Weibull modulus) and s_1 are the shape and scale parameters of the Weibull tail, and μ_G and δ_G are the mean and standard deviation of the Gaussian core ϕ_G if considered extended to $-\infty$; r_f is a scaling parameter required to normalize the grafted cdf such that $\int_{-\infty}^{\infty} p_1(\sigma_N)\mathrm{d}\sigma_N = 1$ Furthermore, continuity of Gaussian and Weibull pdf's at grafting point requires that $\phi_W(\sigma_{N,gr}) = \phi_G(\sigma_{N,gr})$. The cdf of the far-left Weibull tail may be approximated as a power law:

$$P_1 \approx (\sigma_N/s_0)^m \quad \text{and } s_0 = r_f^{1/m}/s_1 \tag{6}$$

For the grafted cdf in Eqs. 4 and 5, the specified grafted point probability P_{gr}, the normalizing condition and the continuity requirements for cdf and pdf represent four constraints. The Weibull tail modulus m must be known (on the basis of tests of very large specimens). To define the grafted cdf uniquely, one needs to know any two of the four statistical parameters, which are μ_G, δ_G, the scale parameter s_1 of Weibull tail, and the normalizing parameter r_f. The calculated statistical parameters, uniquely characterizing the overall cdf, are the grafting stress $\sigma_{N,gr}$, the overall mean μ_0 and the overall standard deviation δ_0.

2.4 Grafted probability distribution for structures of any size

For the purpose of analyzing softening damage and failure, the RVE cannot be defined by homogenization. Rather, it must be defined as the smallest material volume whose failure suffices to cause the whole structure (of positive geometry) to fail (Bažant and Pang 2006, 2007). If one RVE suffices to cause overall failure, the structure must behave as a chain of RVEs. Since the chain survives if all the links survive, the probability of survival of the whole structure is the joint probability of survival of all the RVEs, i.e., $1-P_f=\prod_{i=1}^{N}[1-P_1(\sigma_i)]$ where $P_1(\sigma_i)$ is the failure probability (and $1-P_1$ the survival probability) of the $i-$th RVE subjected to stress σ_i. If the actual number N of RVEs is replaced by the equivalent number N_{eq} modified according to the stress field, all the links in the chain may be considered to have the same stress σ_N and the same cdf, which is $P_1(\sigma_N)$. For the chain, and thus for the quasibrittle structure, one thus gets the failure probability:

$$P_f(\sigma_N)=1-[1-P_1(\sigma_N)]^{N_{eq}} \tag{7}$$

where $N_{eq}=(V/l_0^{n_d})\Psi$

$$\Psi=\int_V \langle\tilde{\sigma}(\xi)\rangle^m \mathrm{d}V(\xi) \tag{8}$$

where $V=$ the volume of the structure, $\langle x\rangle=\max(x,0)$, $l_0=$ RVE size = material characteristic length, $n_d=$ number of dimensions in which the failure is scaled (1, 2, 3), $\xi=$ dimensionless coordinate vector (independent of the structure size), $\tilde{\sigma}=$ dimensionless stress field, and $\Psi=$ dimensionless geometry factor (Bažant and Pang 2007). For small structures ($N_{eq}<5/P_{gr}$) under non-uniform stress, Eq. 7 is not accurate enough as a measure of size. Rather, one must use the joint probability theorem with a recently proposed Boundary layer approach (Bažant et al. 2009).

According to Eq. 7, if the strength of each chain link is Weibullian up to stress $\sigma_{N,gr}$, corresponding to link failure probability $P_1(\sigma_{N,gr})$, then the cdf of the strength of the whole chain is Weibullian for all $P_f\le P_{N,gr}\approx 1-[1-P_1(\sigma_{N,gr})]^{N_{eq}}$. The point $P_{N,gr}$ at the center of the transition from Weibull to Gaussian parts of cdf moves from left to right with increasing structure size, and the transition may approximately be considered as sharp, defined by the aforementioned grafting. For large structures, σ_N is so low that only the far-left cdf tail for each RVE is relevant; thus $P_1(\sigma_N)=(\sigma_N/s_0)^m$, and since $\lim_{N\to\infty}(1+x/N)^N=\mathrm{e}^x$, Eq. 7 yields:

$$P_f(\sigma_N)=1-\left[1-\frac{N_{eq}(\sigma_N/s_0)^m}{N_{eq}}\right]^{N_{eq}} \underset{N_{eq}\to\infty}{\Rightarrow} 1-\mathrm{e}^{-N_{eq}(\sigma_N/s_0)^m} \tag{9}$$

Therefore, the strength distribution for large-size structures must be Weibullian.

For intermediate structure sizes with $N_{eq}<50$, the chance that the minimum RVE strength in the structure will lie in the far-left tail such as $P_f<0.001$ is small. It will likely lie in the end portion of the Gaussian core, typically $0.001<P_f<0.1$, and this is what will decide the structure strength. Therefore, according to the stability postulate of extreme value statistics (and the known domains of attraction of the three possible extreme value distributions (Ang and Tang 1984)), the cdf of an intermediate size structure will approach (in the sense of Barenblatt's intermediate asymptotics (Barenblatt 1996, 2003)) the Gumbel distribution (which was discovered by Fisher and Tippett 1928). But the Gumbelian regime is unimportant because, for larger structures, there is a great chance for the minimum strength to lie in the Weibull tail of one RVE, with $P_f<0.001$. So the final asymptotic cdf will be Weibullian, and neglect of the near Gumbelian intermediate regime appears to be a good approximation.

3 Existing strength histograms on ceramics and their fits with finite threshold

The strength of porcelain was extensively investigated by Weibull (1939). He conducted three-point bend tests

of 102 cylindrical unglazed porcelain rods with diameter 18.6 mm and length 100 mm.

Silicon carbide (SiC) ceramics, which are characterized by very high hardness and wear resistance and are widely used in automotive components, heat exchanger tubes, mechanical seals, etc., were studied by Salem et al. (1996). They tested, under four-point bend loading, 108 prisms of commercially available sintered alpha silicon carbide (Carborundum of Hexoloy, $\alpha-$SiC), with dimensions $2 \times 3 \times 25$ mm; 36 of their prisms were produced with 0° grinding angle without annealing, the next 36 the same but with high temperature annealing, and 36 more with a 90° grinding angle and with high temperature annealing. For all the three groups of 36, they found almost the same strength distribution (Salem et al. 1996).

Silicon nitride ceramics (Si_3N_4) (which were developed in the 1960s and 1970s in a search for dense, high strength and high toughness materials, and are used, e.g., for reciprocating engine components and turbochargers, bearings, and metal cutting or shaping tools) were studied (Santos et al. 2003; Gross 1996; Okabe and Hirata 1995). Gross (1996) conducted four-point bending tests of 27 prismatic beams of sintered silicon nitride (SNW-1000), of dimensions $3.1 \times 4 \times 40.4$ mm. Santos et al. (2003) tested two types of silicon nitride ceramics with performance improving additives: one was a sintering additive ($Si_3N_4 - Al_2O_3 - Y_2O_3$), and another was an aluminum additive (Al_2O_3/Y_2O_3) (which elevates the bending strength and fracture toughness). Santos et al. (2003) further tested 21 four-point bend beams, with dimensions $3 \times 4 \times 45$ mm, made of silicon nitride sintered with rare earth oxide additive ($Si_3N_4 - Al_2O_3 - CTR_2O_3$), which yields similar improvements but at lower costs.

Lanthanum-glass-infiltrated alumina glass ceramics (which are attractive for restorative dentistry due to their aesthetics and bio-compatibility and offer high strength and fracture toughness (Ironside and Swain 1998)) were studied by Lohbauer et al. (2002). They tested alumina-glass composites dry-pressed and pre-sintered $\alpha-Al_2O_3$ with a medium grain size. All alumina were CAD/CAM machined into prisms with dimension $3 \times 4 \times 45$ mm before infiltration with 25% (by weight) of glass of the following weight percentages (Lohbauer 2002): 39–41% of La_2O_3, 16–17% of SiO_2, 15–18% of Al_2O_3, 15% of B_2O_3, 5% of TiO_2 and 4% of CeO_2. 27 four-point bend specimens were tested, under dry condition.

Figure 3 presents six experimentally observed strength histograms of the aforementioned four types of ceramics on the Weibull probability paper. On this paper, the Weibull distribution with zero threshold appears as a straight line of slope m. However, the observed histograms do not appear straight, but exhibit a sharp kink separating two segments, of which the upper one deviates from the straight line. Such deviations have been reported in many studies of ceramics, e.g. (Salem et al. 1996; Okabe and Hirata 1995), and have also been observed for other quasibrittle materials, e.g. concrete (Weibull 1939) and fibrous materials (Wagner 1989; Schwartz 1987), though not for fine-grained perfectly brittle materials at normal laboratory scale.

4 Why must the strength threshold vanish?

4.1 Theoretical argument

According to the present theory, the strength threshold on the atomic lattice scale is zero, and this propagates to the macro-scale of an RVE scale. According to the finite weakest-link model, this property further extends to the structure scale. That the cdf tail on the atomic lattice scale should be a power law with a zero threshold (Eq. 3) follows (1) from the fact that the activation energy barriers for forward and backward jumps on the curve of the free energy potential of atomic lattice block as a function of atomic crack length must differ very little, and (2) from the hypothesis that bridging up the ascending scales is equivalent to some combination of parallel and series couplings. Anyway, it appears impossible to imagine a physical mechanism that would explain how ascending scales could change the threshold to a finite value. Above the RVE scale, preservation of zero threshold is required by the weakest-link model.

4.2 Overall experimental evidence from strength histograms

As an empirical way to fit the histograms, it has recently been widely accepted that the three-parameter Weibull distribution with nonzero threshold σ_u must be used. The histograms from Fig. 3 are re-plotted in Fig. 4 in the scale of $\log(\sigma-\sigma_u)$, and one can see that they indeed become straight. For comparison, the fits of the histograms according to the present theory are also shown,

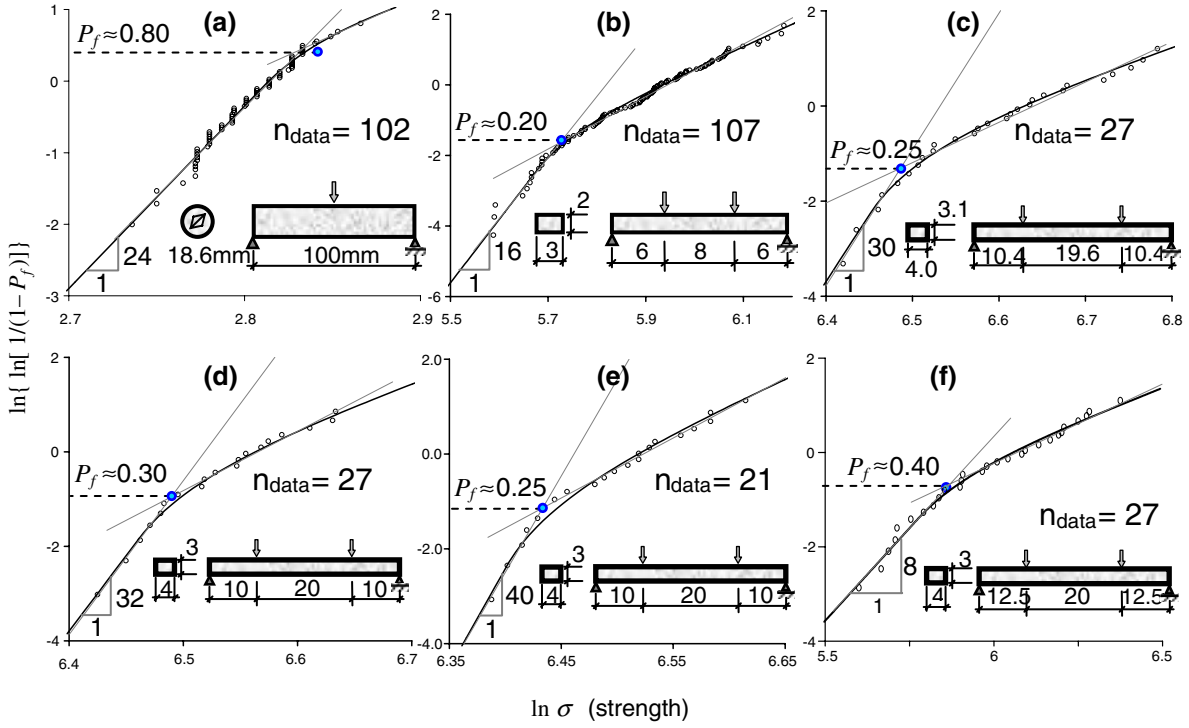

Fig. 3 Optimum fit of strength distribution of ceramics by the present theory: **a** Porcelain, **b** Sintered α − SiC, **c** Sintered Si_3N_4, **d** Sintered $Si_3N_4 - Al_2O_3 - Y_2O_3$, **e** Sintered $Si_3N_4 - Al_2O_3 - CTR_2O_3$, **f** Alumina/glass composite

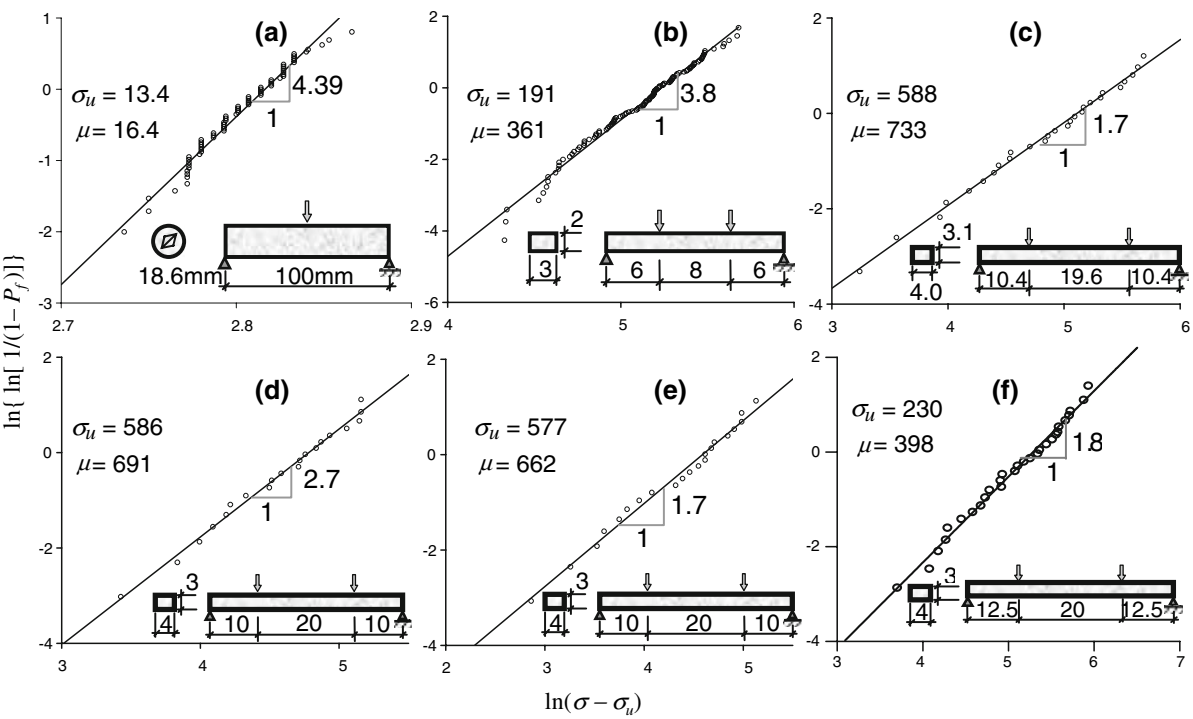

Fig. 4 Histograms in $\log(\sigma - \sigma_u)$ scale

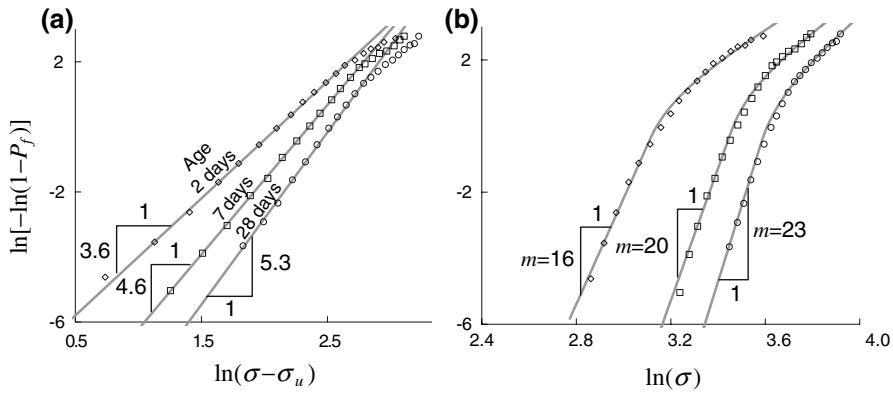

Fig. 5 Optimum fitting of Weibull tests: **a** Weibull cdf's, with finite threshold; **b** chain of RVEs model, with zero threshold

and it is seen that they fit equally well. But are the histograms sufficiently broad to show the difference? They are not.

Significantly broader histograms, consisting of about 2868 data, have been obtained for Portland cement mortar, which is also a quasibrittle material and exhibits virtually the same fracture behavior as tough ceramics; see Weibull's tests (Weibull 1939) in Fig. 5, presented in Weibull scale with zero threshold, for three different ages of mortar, representing three different degrees of chemical hydration. In contrast to Fig. 3, where each point represents just one test, each circle point in Fig. 5 represents the mean strength of a group of about 55 specimens, which is what makes these histograms so smooth and unambiguous.

As seen in Fig. 5, Weibull's broader histograms can again be fitted perfectly by the present model. However, the fit by Weibull distribution with nonzero threshold is less than perfect. Small but systematic deviations are seen at the high probability end (Bažant and Pang 2007). So we must conclude that the overall experimental evidence, as it now exists, mildly favors the zero threshold. A clearer evidence would be desirable because predictions of both theories for very low failure probabilities such as $P_f = 10^{-6}$, which matter for practical design, are very different.

Figure 6 shows the prediction of safety factors for six aforementioned ceramics materials by the present theory, three-parameter Weibull distribution and Gaussian distribution. Comparing the present theory and the three-parameter Weibull model, the safety factors for loads corresponding to $P_f = 10^{-6}$ can differ by a factor as large as 3.4. Such a large difference is due to a relatively low Weibull modulus for alumina/glass ceramics. A residual porosity of the infiltration process might be responsible for the scatter of the strength. But to make the experimental evidence from histograms unambiguous, a forbidding amount of testing would be needed. Therefore, one must seek and analyze experimental evidence for other predictions of the theory. Among these, the size effect is the most effective.

4.3 Consequence of mean size effect tests

Unfortunately, the histograms in Figs. 3 and 5 were all tested for one specimen size. If they were tested for two significantly sizes differing by a ratio of at least 4, the discrepancy between the zero and non-zero thresholds would get manifested clearly.

The straight lower left segment of the typical histograms seen in Fig. 3 can be fitted by the Weibull distribution with a zero threshold. A linear regression can be used for that. According to the present theory, the upper right segment may, for a sufficiently small structure ($N < 10$), be fitted by a straight line if the histogram data are transferred to the normal probability paper. This can again be done by linear regression. Transferring this straight line back into the Weibull paper, one gets a curve, and its intersection with the Weibull straight line for the lower part gives the precise position of the kink point, which is also the correct position of the grafting point; see Fig. 3.

Now the important point to note is that, for quasibrittle materials, modeled by a finite chain with a finite RVE size, the kink point (or grafting point) moves rapidly upward as the number N of RVEs in the chain increases. Since the survival probability at each kink point must be equal to the joint survival probability of all N_{eq} RVEs subjected to the same σ_N, the kink point location (or the terminal point of Weibull segment of cdf) may be calculated as

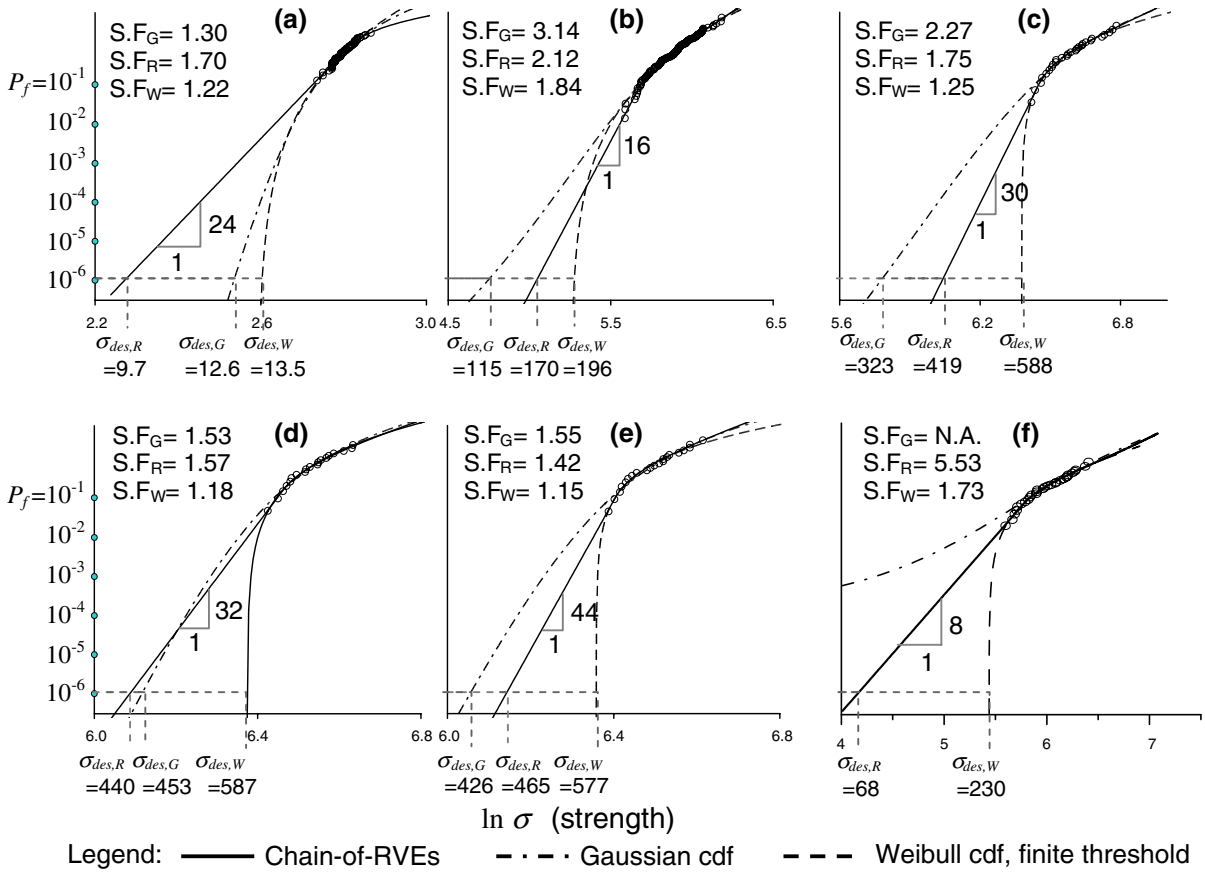

Fig. 6 Prediction of safety factors of ceramics by the present theory, three-parameter Weibull distribution, and Gaussian distribution

$$P_{f,gr}(\sigma_N) = 1 - [1 - P_1(\sigma_{1,gr})]^{N_{eq}} \tag{10}$$

where $\sigma_N = \sigma_{1,gr}$ and $P_1(\sigma_{1,gr})$ is the maximum failure probability at which the power-law tail of one RVE still applies (which is the grafting point probability for one RVE, i.e. for $N_{eq} = 1$). If $P_1(\sigma_{1,gr}) \approx 0.001$, then for $N_{eq} = 10, 100, 300$ and $1{,}000$ the kink point of cdf lies at $P_{f,gr} = 1\%, 9\%, 26\%$ and 63%, respectively. For $N_{eq} = 5{,}000$, it moves above 99.3%, which is outside the practical range, and the cdf is then totally Weibullian.

Consider now the size extrapolation of the histograms according the present theory and the three-parameter Weibull model with nonzero threshold; see Fig. 7. As the diagrams show for the larger structure, while the three-parameter Weibull model predicts the distribution poorly for the low probability range, it does so quite well for the high probability range. However, for the three-parameter Weibull cdf to yield a close fit of the histogram for a large (though not too large) structure, it would be necessary to allow Weibull modulus m to take different values for different sizes.

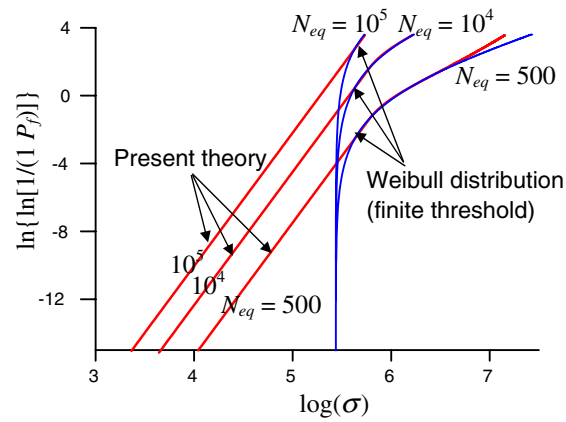

Fig. 7 Size extrapolation of histograms

But this would be physically inadmissible since the Weibull modulus is an atomistically based property of the tail of cdf of RVE strength, and thus a material constant. It cannot depend on the size (nor the geometry) of the structure (in spite of contrary suggestions in the recent literature).

Unfortunately, testing for the size effect did not accompany the histogram testing of ceramics shown in Fig. 3. According to the present theory, if the histograms were tested for at least two significantly different sizes of geometrically similar specimens, one could clearly distinguish the two theories on the basis of the kink point location.

A clear distinction between the three-parameter Weibull theory and the present theory can be obtained even more efficiently, with fewer specimens, by testing the size effect merely for the mean nominal strength. Although, in this case, a broader size range, spanning the size ratio of at least 1:8 (with at least four different sizes), is required, only 3–6 specimen per size should suffice (depending on scatter width). The key feature of the size effect curve (of unnotched specimens, failing at macro-crack initiation from an RVE at specimen surface) is a deviation from the power-law large-size asymptote of Weibull statistical size effect (Fig.9c of Bažant and Pang 2007). This deviation is centered at the point where $P_{f,gr} = 50\%$. The corresponding value of N_{eq} should lie roughly in the middle of the size range of specimens (in the logarithmic scale), in order to capture the size at which the deviation takes place (this value of N_{eq} is 693 for $P_1(\sigma_{1,gr}) = 0.001$, and 69 for $P_1(\sigma_{1,gr}) = 0.01$).

For one and the same quasibrittle material, test data of sufficiently broad size range do not exist at present. Nevertheless, there exist many narrower-range size effect data obtained with different types of concrete. When they are combined in one dimensionless size effect plot, the resulting optimum fit does indeed show a deviation from the Weibull power-law asymptote, as shown in a plot of $\log \sigma_N$ versus $\log D$ where $D =$ characteristic specimen size (see Fig. 2 in Bažant and Novák 2000b).

This experimental evidence of the deviation from power-law size effect is further reinforced by the fact that the same mean size effect diagram has also been obtained by Monte Carlo simulation according to the nonlocal generalization of Weibull statistical theory (Bažant and Xi 1991); see Fig. 5b in Bažant et al. 2007 (this is a simpler theory than the present one, giving about the same results for the central range of cdf, but inapplicable to the cdf tails).

If the pdf of one RVE, denoted as $p_1(\sigma_N)$, is known, the mean size effect curve according to the weakest-link model may be computed by numerical evaluation of the integral:

$$\bar{\sigma}_N = \int_0^\infty [1 - P_f(\sigma_N)]\mathrm{d}\sigma_N \tag{11}$$

Computation of this integral not only confirms that onset of the deviation of the size effect curve from the power-law size effect of Weibull statistical theory is determined by the grafting point probability, but also shows that the steepness of the deviation is governed by the coefficient of variation of single RVE strength (Bažant and Pang 2007).

As a further, indirect, support of the present theory, it may be pointed out that the curve of size effect on the mean strength according to Eq. (11) matches the type I energetic-statistical size effect law (Bažant and Pang 2007; Bažant 2004a; Bažant 2004b):

$$\sigma_N = \sigma_0 \left[\left(\frac{D_b}{D} \right)^{rn/m} + \frac{r D_b}{D} \right]^{1/r} \tag{12}$$

where σ_0, D_b and r are positive constants to be determined by experiments. This law, whose deviation from the Weibull power-law size effect is caused by the finite size of the fracture process zone, was derived by three independent ways: (1) from the limit of cohesive fracture mechanics for vanishing crack length; (2) from the stress redistribution caused by a large fracture process zone formed at structure surface; and also (3) from the aforementioned nonlocal generalization of Weibull theory (Bažant and Xi 1991, Bažant and Novák 2000a; Bažant 2004a). This law has been shown to fit closely the size effect tests of mean flexural strength of various quasibrittle structures (Bažant and Xi 1991; Bažant 2004a; Bažant 2004b). These agreements again support the present theory, which in turn rules out the possibility of nonzero threshold for quasibrittle structures. The physical reason for the deviation of size effect from the Weibull power law is for all these approaches the same—the non-negligible size of the fracture process zone, or of the RVE.

For comparison, let us now calculate, according to the weakest-link model (Eq.10), the mean size effect curve when the three-parameter Weibull model is extrapolated from size D_0 (corresponding to N_{eq1}) to

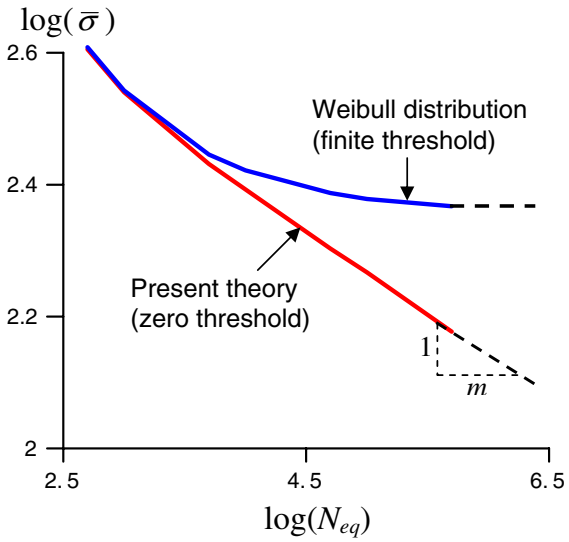

Fig. 8 Size effect curve on mean strength

size D (corresponding to N_{eq});

$$\bar{\sigma}_N = \int_0^\infty (1 - P_f)\mathrm{d}\sigma_N \tag{13}$$

$$= \int_0^\infty (1 - P_{f1})^{N_{eq}/N_{eq1}}\mathrm{d}\sigma_N \tag{14}$$

$$= \int_0^\infty \left[\exp\left(-\left\langle\frac{\sigma_N - \sigma_0}{s_0}\right\rangle^m\right)\right]^{N_{eq}/N_{eq1}} \mathrm{d}\sigma_N \tag{15}$$

$$= \sigma_0 + s_0\Gamma\left(1 + \frac{1}{m}\right)\left(\frac{N_{eq1}}{N_{eq}}\right)^{1/m} \tag{16}$$

Figure 8 presents the size effect curves predicted from the present theory and from the three-parameter Weibull theory with nonzero threshold. The size effect curves predicted by the latter and the former agree well only in the size range for which the experimental histograms have been reported, which is expected since both have been shown to fit these histograms well. However, these two theories begin to deviate for larger structures. The mean strength for the present theory converges for large sizes to the a power-law size effect of two-parameter Weibull theory with zero threshold, while the mean strength curve extrapolating the three-parameter Weibull model has (in a log–log plot) a gradually diminishing slope and for large sizes asymptotically converges to a constant, σ_0. These are incorrect features, which alone suffice to invalidate the hypothesis of nonzero threshold.

Here we see that tests of the size effect on mean strength can be used to test the soundness of a crucial hypothesis about probability distribution of strength. This is an attractive alternative to the testing of strength histograms, which represents a tedious and costly experimental effort since, for each structure size, one may need to prepare and test several hundred specimens, and even that does not suffice to reveal the tail of probability distribution. Also, histogram testing has the disadvantage that the low probability range is very sensitive to inevitable experimental errors that can greatly affect the distribution tail. By contrast, mere 3 to 6 specimens for each of about four different sizes suffice for give the size effect curve, from which the main features of strength distribution (exponent m, coefficient of variation and grafting probability) can be identified.

5 Combining strength histograms for different structure sizes and geometries

Equation (7) implies that if sets of strength data for specimens of different sizes (and possibly different geometries) are plotted in the diagram of Y versus X, in which

$$Y = \ln[-\ln(1 - P_f)] - \ln N_{eq} \tag{17}$$

$$X = \ln\{-\ln[1 - P_1(\sigma_N)]\} \tag{18}$$

then the strength data for all the sizes (and geometries) should coalesce into one histogram (or one curve), provided that the weakest-link model is applicable (and that N_{eq} can be approximately calculated from Eq. 8 based on LEFM). In the regular Weibull probability paper, the histogram for N_{eq1} should become coincident with the histogram for N_{eq2} after a vertical shift through the distance $\ln(N_{eq2}) - \ln(N_{eq1})$.

For σ_N values $< \sigma_{1,gr}$ for which the left tail of $P_1(\sigma_N)$ is Weibullian, we may set $P_1(\sigma_N) = 1 - \mathrm{e}^{-(\sigma_N/s_0)^m}$, and algebraic rearrangement of the last equation then leads to the linear regression equation $Y = mX + C$ where

$$X = \ln\sigma_N, \quad C = -m\ln s_0 \tag{19}$$

So, for $\sigma_N < \sigma_{1,gr}$, the histograms for different specimen sizes (and shapes) must in this kind of plot fuse into one straight line up to the kink point at $\sigma_N = \sigma_{1,gr}$, provided that the weakest-link model is valid and that the tail of P_1 is Weibullian up to $\sigma_N = \sigma_{1,gr}$.

Statistical analysis of data from various specimen sizes and shapes is, in these particular X and Y coordinates, quite easy. For determining the material parameters m, s_0 and $\sigma_{1,gr}$, this approach is statistically more effective that using the mean size effect curve and the strength histograms separately. Regrettably, at present there are no data in the literature to check this approach.

6 Concluding remark

Switching from nonzero to zero threshold may often cause a great change in the safety factor required to ensure that $P_f < 10^{-6}$. But not always. On the cdf of strength, to be sure, the distance from the mean to the point of $P_f = 10^{-6}$ will increase several fold in terms of standard deviations. However, that does not necessarily cause a several fold increase of the safety factor, because the coefficient of variation of strength may decrease significantly with the structure size if the behavior is quasibrittle rather than brittle. Sometimes this opposite effect may completely offset the effect of the increased relative distance from the mean.

References

Ang AH-S, Tang WH (1984) Probability concepts in engineering planning and design. vol II. Decision, risk and reliability. Wiley, New York

Barenblatt GI (1996) Scaling, selfsimilarity and intermediate asymptotics. Cambridge University Press, (Cambridge, UK)

Barenblatt GI (2003) Scaling. Cambridge University Press, (Cambridge, UK)

Bažant ZP (1984) Size effect in blunt fracture: concrete, rock, metal. J Eng Mech, ASCE 110(4):518–535

Bažant ZP (2001) Size effects in quasibrittle fracture: Aperçu of recent results. In: de Borst R, Mazars J, Pijaudier-Cabot G, van Mier JGM (eds) Fracture mechanics of concrete structures (Proc., FraMCoS-4 Int. Conf., Paris), Swets & Zeitlinger, A.A. Balkema Publishers, Lisse, 651–658

Bažant ZP (2004a) Probability distribution of energetic-statistical size effect in quasibrittle fracture. Probab Eng Mech 19(4):307–319

Bažant ZP (2004b) Scaling theory for quasibrittle structural failure. Proc Natl Acad Sci USA 101(37):13397–13399

Bažant ZP (2005) Scaling of structural strength. 2nd edn. Elsevier, London

Bažant ZP, Chen E-P (1997) Scaling of structural failure. Appl Mech Rev ASME 50(10):593–627

Bažant ZP, Kazemi MT (1990) Size effect in fracture of ceramics and its use to determine fracture energy and effective process zone length. J Am Ceram Soc 73(7):1841–1853

Bažant ZP, Novák D (2000a) Probabilistic nonlocal theory for quasibrittle fracture initiation and size effect. I. Theory. II. Application. J Eng Mech ASCE 126(2):166–185

Bažant ZP, Novák D (2000b) Energetic-statistical size effect in quasibrittle failure at crack initiation. ACI Mater J 97(3):381–392

Bažant ZP, Pang S-D (2005) Revision of reliability concepts for quasibrittle structures and size effect on probability distribution of structural strength. In: Augusti G, Schuëller GI, Ciampoli M (eds) Safety and reliability of engrg. systems and structures (Proc., 8th Int. Conf. on Structural Safety and Reliability, ICOSSAR 2005, held in Rome), Millpress, Rotterdam, pp 377–386

Bažant ZP, Pang S-D (2006) Mechanics-based statistics of failure risk of quasibrittle structures and size effect on satety factors. Proc Natl Acad Sci USA 103(25):9434–9439

Bažant ZP, Pang S-D (2007) Activation energy based extereme value statistics and size effect in brittle and quasibrittle fracture. J Mech Phys Solids 32(55):91–131

Bažant ZP, Planas J (1998) Fracture and size effect in concrete and other quasibrittle materials. CRC Press, Boca Raton and London

Bažant ZP, Xi Y (1991) Statistical size effect in quasi-brittle structures: II. Nonlocal theory. J Eng Mech ASCE 117(17):2623–2640

Bažant ZP, Vořechovský M, Novák D (2007) Asymptotic prediction of energetic-statistical size effect from deterministic finite element solutions. J Eng Mech ASCE 128:153–162

Bažant ZP, Le J-L, Bazant MZ (2008) Size effect on strength and lifetime distributions of quasibrittle structures implied by interatomic bond break activation. Proc. 17th Eur. Conf. on Fracture. (held in Brno, Sept. 2008) (in press)

Bažant ZP, Le J-L, Bazant MZ (2009) Scaling of strength and lifetime distributions of quasibrittle structures based on atomistic fracture mechanics. Theoretical & Appl Mech Rep No 08-12/C6055, Northwestern Univ. Submitted to Proc Natl Acad Sci USA

Bulmer MG (1979) Principles of statistics (chapter 12). Dover Publ., New York

Bouchaud J-P, Potters M (2000) Theory of financial risks: from statistical physics to risk management. Cambridge University Press, Cambridge, UK

Daniel HE (1945) The statistical theory of the strength of bundles and threads. Proc R Soc Lond 183:405–435

Duckett K (2005) Risk analysis and the acceptable probability of failure. Struct Eng 83(15):25–26

Duffy SF, Powers LM, Starlinger A (1993) Reliability analysis of structural ceramic components using a three-parameter Weibull distribution. Trans ASME J Eng Gas Turbines Power 115:109–116

Eyring H (1936) Viscosity, plasticity and diffusion as examples of absolute reaction rates. J Chem Phys 4:283–291

Fisher RA, Tippett LHC (1928) Limiting forms of the frequency distribution of the largest and smallest member of a sample. Proc Camb Philol Soc 24:180–190

Freudenthal AM (1968) Statstical approach to brittle fracture. In: Lievowitz H. (ed) Fracture: an advanced treatise. Academic Press, New York, vol 2 pp 591–619

Gross B (1996) Least squares best fit method for the three parameter weibull distribution: analysis of tensile and bend specimens with volume or surface flaw failure. NASA TM-4721 pp 1–21

Gumbel EJ (1958) Statistics of extremes. Columbia University Press, New York

Harlow DG, Smith RL, Taylor HM (1983) Lower tail analysis of the distribution of the strength of load-sharing systems. J Appl Probab 20:358–367

Ironside JG, Swain MV (1998) Ceramics in dental restorations—a review and critical issues. J Aust Ceram Soc 34(2):78–91

Kaxiras E (2003) Atomic and electronic structure of solids. Cambridge University Press, Cambridge

Lohbauer U, Petchelt A, Greil P (2002) Lifetime prediction of CAD/CAM dental ceramics. J Biomed Mater Res 63(6):780–785

Melchers RE (1987) Structural reliability, analysis & prediction. Wiley, New York

NKB (Nordic Committee for Building Structures) (1978) Recommendation for loading and safety regulations for structural design. NKB Report, No. 36

Okabe N, Hirata H (1995) High temperature fatigue properties for some types of SiC and Si_3N_4 and the unified strength estimation method. In: Kishimoto H, Hoshide T, Okabe N (eds) Cyclic fatigue in ceramics. Elsevier Science B. V. and The Society of Materials Science, Japan pp 245–276

Philips R (2001) Crystals, defects, and microstructures: modeling across scales. Cambridge University Press, Cambridge

Phoenix SL, Ibnabdeljalil M, Hui C-Y (1997) Size effect in the distribution of strength of brittle matrix fibrous composites. Int J Solids Struct 34(5):545–568

RILEM TC QFS (chaired by Z.P. Bažant) (2004) Quasibrittle fracture scaling and size effect—Final report. Mater Struct (Paris) 37(272):547–586

Risken H (1989) The Fokker–Planck equation. 2nd edn. Springer Verlag, Berlin

Salem JA, Nemeth NN, Powers LP, Choi SR (1996) Reliability analysis of uniaxially ground brittle materials. J Eng Gas Turbines Power 118:863–871

Santos Cd, Strecker K, Piorino Neto F, de Macedo Silva OMM, Baldacum SA, de Silva CRM (2003) Evaluation of the reliability of $Si_3N_4-Al_2O_3-CTR_2O_3$ ceramics through Weibull analysis. Mater Res 6(4):463–467

Schwartz P (1987) A review of recent experimental resulst concerning the strength and time dependent behaviour of fibrous poly (Paraphenylene Terephthalamide). Polym Eng Sci 27(11):842–847

Stanley P, Inanc EY (1985) Assessment of surface strength and bulk strength of a typical brittle material. In: Eggwertz S, Lind NC (eds) Probabilistic methods. I. The mechanics of solids and structures. Springer-Verlag, Berlin pp 231–251

Wagner HD (1989) Stochastic concepts in the study of size effects in the mechanical strength of highly oriented polymeric materials. J Polym Sci 27:115–149

Weibull W (1939) The phenomenon of rupture in solids. Proceedings of Royal Swedish Institute of Engineering Research, Stockholm, 151:1–45